J. Radiat. Res., 50, 407–413 (2009)

Review

An Approach to Estimate Radioadaptation from DSB Repair Efficiency#

Fumio YATAGAI[1]*, Kaoru SUGASAWA[2], Shuichi ENOMOTO[1] and Masamitsu HONMA[3]

Radioadaptation/I-SceI digestion/DSB repair/TK6 cells.

In this review, we would like to introduce a unique approach for the estimation of radioadaptation. Recently, we proposed a new methodology for evaluating the repair efficiency of DNA double-strand breaks (DSB) using a model system. The model system can trace the fate of a single DSB, which is introduced within intron 4 of the *TK* gene on chromosome 17 in human lymphoblastoid TK6 cells by the expression of restriction enzyme I-SceI. This methodology was first applied to examine whether repair of the DSB (at the I-SceI site) can be influenced by low-dose, low-dose rate gamma-ray irradiation. We found that such low-dose IR exposure could enhance the activity of DSB repair through homologous recombination (HR). HR activity was also enhanced due to the pre-IR irradiation under the established conditions for radioadaptation (50 mGy X-ray–6 h–I-SceI treatment). Therefore, radioadaptation might account for the reduced frequency of homozygous loss of heterozygosity (LOH) events observed in our previous experiment (50 mGy X-ray–6 h–2 Gy X-ray). We suggest that the present evaluation of DSB repair using this I-SceI system, may contribute to our overall understanding of radioadaptation.

INTRODUCTION

It is important to accurately estimate human health risks for persons occupationally exposed to ionizing radiation (IR), such as airline crews and workers in medical and industrial fields. For estimating such risks, it is worthwhile to investigate radioadaptation, that is, acquiring a cellular radioresistance to a challenging IR by a pre-exposure to low-dose IR. Radioadaptation was first reported by Olivieri *et al.*[1] The priming radiation exposure delivered by labeling human lymphocytes with tritiated thymidine caused a decrease in chromosomal aberration frequency after a challenging exposure to 1.5 Gy of IR. That discovery stimulated a series of studies using human lymphocytes and various mammalian cell lines as described in reviews.[2,3] A reduced induction of both micronuclei and sister chromatid exchanges was shown in Chinese hamster V79 cells pre-exposed to low doses of γ-rays or ^{3}H β-rays.[4] Subsequent studies reported similar radioadaptive responses, such as reduced mutation frequencies in human lymphocytes,[5] mouse SR-1 cells[6] and human-hamster hybrid A_L cells,[7] an altered mutation spectrum in human-hamster hybrid A_L cells,[7] reduced micronucleus frequencies in human lymphocytes[8] and mouse embryo cells,[9] and reduced deletions and rearrangements in human lymphoblast cells.[10] Those studies suggest that radioadaptation is an important defense mechanism against a high-dose IR, although the molecular mechanisms involved remain largely unknown.[11–15]

Cellular responses such as a bystander effect, genetic instability, and hyper-radiosensitivity are reported to be tightly related to the radioadaptation.[16–21] In mammalian cells, for example, bystander mutagenesis may be suppressed by an adaptive response.[16] Another example is the possible involvement of a "radioadaptive bystander" effect in human lung fibroblasts.[22] The reduction of radiosensitivity in cells with a wild type *p53* gene by a radiation-induced, nitric oxide (NO)-mediated bystander effect may also be a manifestation of the radioadaptation.[21,23] This possibility is supported by the finding that the NO-induced apoptosis observed in lymphoblastoid and fibroblast cells depends on the phosphorylation and activation of p53.[24] In fact, p53 was suggested to play a key role in the mechanisms of an adaptive response

*Corresponding author: Phone: +81-48-467-9710,
Fax: +81-48-467-9710,
E-mail: yatagai@riken.jp

[1]Metallomics Imaging Research Unit, Center for Molecular Imaging Science, The Institute of Physical and Chemical Research (RIKEN), Saitama 351-0198, Japan; [2]Biosignal Research Center, Kobe University, Hyogo 657-8501, Japan; [3]Division of Genetics and Mutagenesis, National Institute of Health Sciences, Tokyo 158-8501, Japan.

#Translated and modified from Radiat. Biol. Res. Comm. Vol.43(4); 443–453, (2008, in Japanese).
doi:10.1269/jrr.09050

mediated by a feedback signaling pathway involving protein kinase C (PKC), p38 mitogen activated protein kinase (p38MAPK), and phospholipase C (PLC).[11,13,25]

One of the possible targets for radioadaptation is oxidative base damage. A low-dose rate whole body γ-irradiation of mice (1.2 mGy/h, total 0.5 Gy) demonstrated the activation of antioxidative enzymes such as MnSOD and catalase in spleen cells, leading to less DNA damage as determined by a comet assay.[26] Furthermore, down-regulation of the human *CDC16* gene that occurs after oxidative stress causes more rapid and efficient repair in adapted (2 cGy pre-irradiated) human lymphoblastoid cells challenged with 4 Gy irradiation.[12] However, oxidative base excision repair enzymes, including DNA glycosylases, hOGG1, and hNth1, are reportedly not up-regulated at the post-transcriptional level in γ-ray-primed TK6 cells.[27] Those reports suggest that the antioxidant defense machinery is likely to be involved in radioadaptation although the mechanisms involved are still not well understood.

Gene expression also seems to be tightly related to a variety of functions in the adaptive response such as the induction of antioxidant defense machinery, repair of DNA damage, control of cell-cycle progression, *etc.* In fact, *de novo* synthesis of transcripts and proteins is reported to be required for the expression of the adaptive response.[28] Following that report, gene expression analysis has been extensively studied by many investigators.[15,28–31] For example, the *CHD6* gene in human lymphoblastoid cell AHH-1 can be up-regulated by 0.5 Gy of γ-irradiation and its induced expression could be involved in a low-dose hypersensitive response.[29] Recently, gene profiles in the kidney and testis from γ-irradiated (485 days at dose rates of 0.032–13 μGy/min) mice were determined using oligonucleotide microarrays, and differentially expressed genes were identified.[31]

DNA double strand breaks (DSBs) are a most serious type of DNA damage. They can be caused by IR or radiomimetic chemicals, and they can occur spontaneously during DNA replication. The nonrepair or misrepair of DSBs can cause cell death or mutagenic and/or carcinogenic consequences, so the accurate repair of DSBs is important for maintaining genomic integrity.[32,33] In other words, DSB repair is an essential function in all living organisms. Recently analyses using nondividing lymphocyte and fibroblast cells suggested that the adaptive response is not mediated by an enhanced rejoining of DNA strand breaks but rather is a reflection of perturbation in cell cycle progression.[34] On the other hand, the induction of an efficient chromosome repair system by the priming radiation dose is considered to be involved in radioadaptation mechanisms, and in fact, the efficiency of DSB repair in Chinese hamster V79 cells exposed to γ-rays is enhanced by a priming exposure of 5 cGy of γ-rays.[35] The reduced frequencies of chromosomal alterations as described above supports the latter possibility of DSB-repair enhancement. At the present stage, it is difficult to conclude which factor, cell-cycle perturbation or DSB repair, largely contributes to radioadaptation.

THE I-SCEI SYSTEM FOR DSB REPAIR EVALUATION

Outline of the system

A model system was constructed for evaluating DSB repair by tracing the fate of a single DSB on chromosomal DNA. The DSB generated in this system can be considered as a target DNA-lesion susceptible to repair, and this system can distinguish two major DSB repair pathways, non-homologous end-joining (NHEJ) and homologous recombination (HR) (Fig. 1).[36,37] The human lymphoblastoid cell line TSCE5 is heterozygous (+/–) for the thymidine kinase (*TK*) gene and the line TSCER2 is compound heterozygous (–/–; two different TK^- alleles); both carry an I-SceI endonuclease recognition site in intron 4 on one allele of the *TK* gene. DSBs can be generated at the I-SceI site by expression of the I-SceI vector.[36,37] When DSBs occur at the *TK* locus, NHEJ in TSCE5 cells produces TK-deficient mutants while HR between the *TK* alleles in TSCER2 cells produces TK-proficient revertants. This means that positive-negative drug selection for TK phenotypes permits distinction between NHEJ and HR repair.

Cell line construction for use in the system

Details of the strain construction are described in our previous work (Fig. 2).[36] Briefly, in lymphoblastoid TK6 cells heterozygous for the *TK* gene, the functional allele was first inactivated by gene targeting with vector pTK4 to

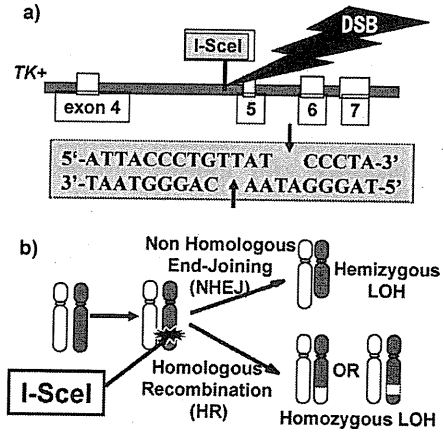

Fig. 1. Principle of DSB formation and repair evaluation. A single DNA double strand break (DSB) is generated at the I-SceI recognition site in a human lymphoblastoid TK6 cell by transfecting an I-SceI expression vector (a) and the efficiencies of DSB repair through non-homologous end-joining (NHEJ) or homologous repair (HR) are evaluated from induction of hemizygous and homozygous LOH events, respectively (see text).

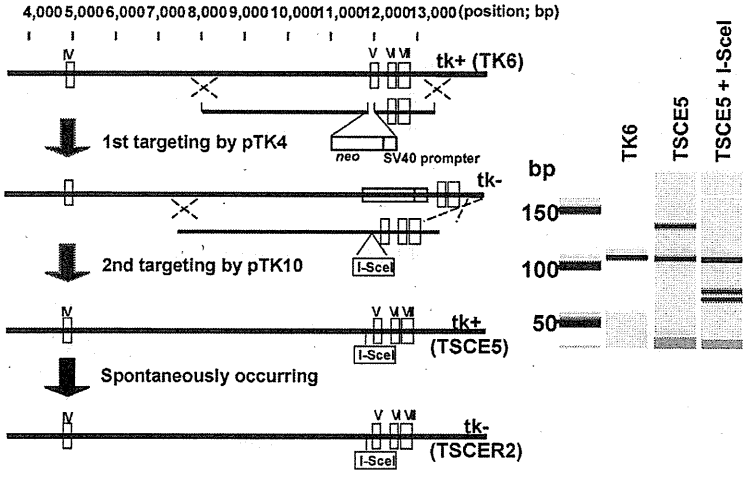

Fig. 2. Cell line construction. In the TK6 cell line, the functional allele of *TK* gene was first inactivated by gene targeting vector pTK4 and then the I-SceI recognition site was introduced at 75 bp upstream of exon 5 in the *TK* gene. The new line was termed TSCE5 and its compound heterozygote (*TK*–/–) cell line, TSCER2, was also isolated (see text).

replace exon 5 of the *TK* gene by a *neo* gene. To introduce the I-SceI recognition site at 75 bp upstream of exon 5, the targeting vector pTK10, encompassing about 6 kb of the original *TK* gene with exons 5, 6, and 7, and the I-SceI recognition site in intron 4, was used to revert the *TK* gene disrupted by pTK4. The new line was termed TSCE5. A spontaneous mutation in a TSCE5 cell (G to A in position 23 of exon 5), which we cloned, led to the compound heterozygote (*TK*–/–) cell line, TSCER2.

I-SceI expression for introduction of DSB

We introduced the I-SceI expression vector (pCBASce) by electroporation methodology using Nucleofector Kit V (amaxa AG, Cologne, Germany) (Fig. 3).[36–38] The I-SceI expression vector was introduced into about 65% of the cells at 24 hr after the transfection and the expression last for 3 days incubation.[37] The relatively long expression allowed us to succeed in estimating the influence of low-dose, low-dose-rate γ-rays irradiation on DSB repair, especially the effect of post-IR-exposure, as described below.

Evaluation of DSB repair efficiencies

Measurements of TK^- mutants and TK^+ revertants allow us to evaluate DSB repair efficiencies through NHEJ and HR pathways, respectively (Fig. 3). In TSCE5, when a DSB at the I-SceI site is repaired by NHEJ involving a deletion in the adjacent exon, the cell can be isolated as a TK-deficient mutant. In TSCER2, when a DSB is repaired by HR between the *TK* alleles, a TK^+ allele can be generated, resulting in a revertant phenotype. The DSB repair *via* NHEJ was 73–86 times higher than that *via* HR in our previous studies.[36,37] These findings are consistent with the report that NHEJ is the major repair pathway in mammalian cells.[39]

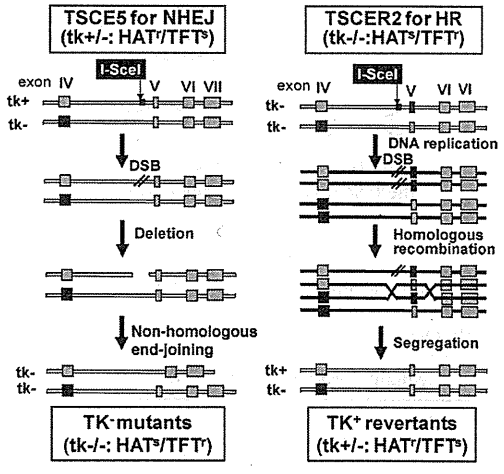

Fig. 3. An approach to evaluate DSB repair efficiency. In TSCE5, when a DSB at the I-SceI site is repaired by NHEJ involving a deletion in the adjacent exon, the cell can be isolated as a TK-deficient mutant. In TSCER2, when a DSB is repaired by HR between the *TK* alleles, a TK^+ allele can be generated, resulting in a revertant phenotype (see text). Filled exons represent TK mutations.

APPLICATION OF THE I-SCEI SYSTEM FOR EVALUATING RADIOADAPTATION IN TERMS OF DSB REPAIR

Influence of low-dose, low-dose-rate γ-rays on DSB repair

The I-SceI digestion system was applied for estimating the influence of low-dose, low-dose-rate γ-irradiation on repair of a site-specifically introduced DSB (Fig. 4).[38] The results

obtained with Mode A (30 mGy of pre-γ-irradiation) and Mode B (8.5 mGy of post-γ-irradiation) are shown in Tables 1 and 2, respectively. The NHEJ repair of DSB was little influenced by either modes of low-dose, low dose-rate γ-irradiation. DSB repair by HR, in contrast, was enhanced by ~50% and ~80% in Mode A and Mode B, respectively. This might implicate that both pre-γ-irradiation (Mode A) and post-γ-irradiation (Mode B) induce a radioadaptation, although both modes of irradiations, especially Mode B, are different from the original concept of radioadaptation. In fact, DSBs are generated during the γ-irradiation in Mode B, because I-SceI expression lasts for 3 days incubation as previously mentioned.

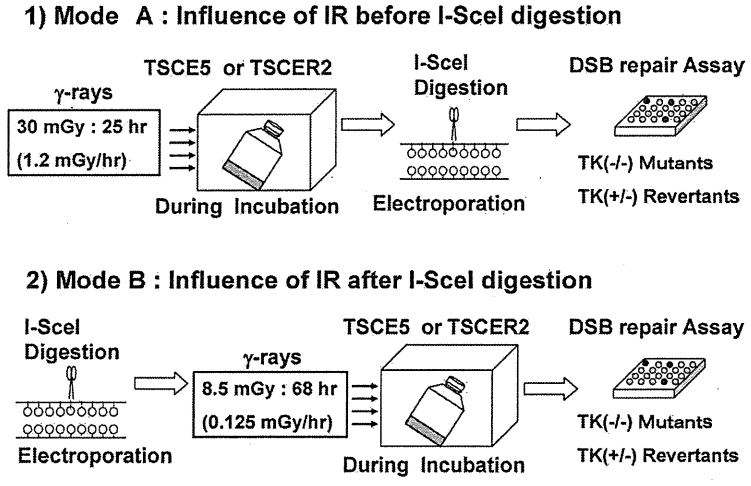

Fig. 4. Influence of low-dose IR exposure on DSB repair. Experimental schemes of radiation exposure and I-SceI expression are illustrated. Mode A: cells were exposed to low-dose, low-dose-rate γ-rays and then transfected with the I-SceI vector by electroporation (see text). 2) Mode B: cells were transfected with the I-SceI vector and then exposed to γ-rays at a much lower dose and dose-rate (see text).

Table 1. Effect of pre-IR exposure on DSB repair (Mode A).

a) NHEJ efficiency in TSCE5 cells

Exp.	Mutant Frequency, MF ($\times 10^{-6}$)				Effect of IR (Relative MF*)
	Control	γ-rays	I-SceI	γ-rays + I-SceI	
1	3.5	6.1	8600	8500	0.99
2	1.8	3.2	2900	3200	1.1
Average	2.7	4.7	5800	5900	1.0 (P = 0.82)

*Relative MF was calculated as MF (γ-rays + I-SceI)/MF (I-SceI).

b) HR efficiency in TSCER2 cells

Exp.	Revertant Frequency, RF ($\times 10^{-6}$)				Effect of IR (Relative RF*)
	Control	γ-rays	I-SceI	γ-rays + I-SceI	
1	–	–	90	114	1.3
2	–	–	62	96	1.5
3	–	–	25	45	1.8
Average	–	–	59	85	1.5 (P = 0.021)

*Relative RF was calculated as RF (γ-rays + I-SceI)/RF (I-SceI).

Table 2. Effect of post-IR exposure on DSB repair (Mode B).

a) NHEJ efficiency in TSCE5 cells

Exp.	Mutant Frequency, MF ($\times 10^{-6}$)				Effect of IR (Relative MF*)
	Control	γ-rays	I-SceI	γ-rays + I-SceI	
1	2.8	1.3	3400	4500	1.3
2	3.1	2.8	12000	17000	1.4
3	–	–	11000	11000	1.0
Average	3.0	2.1	8800	10800	1.2 (P = 0.12)

*Relative MF was calculated as MF (γ-rays + I-SceI)/MF (I-SceI).

b) HR efficiency in TSCER2 cells

Exp.	Revertant Frequency, RF ($\times 10^{-6}$)				Effect of IR (Relative RF*)
	Control	γ-rays	I-SceI	γ-rays + I-SceI	
1	–	–	82	160	2.0
2	–	–	160	270	1.7
3	–	–	110	190	1.7
Average	–	–	120	210	1.8 (P = 0.0013)

*Relative RF was calculated as RF (γ-rays + I-SceI)/RF (I-SceI).

Influence of low-dose X-ray irradiation on DSB repair

We have extensively studied the effects of low-dose IR by using a loss of heterozygosity (LOH) analysis system.[40–42] The thymidine kinase deficient (TK^-) mutants induced in TK6 cells can be classified as LOH type and non-LOH type by this system. The LOH mutants were further classified as homozygous-type and hemizygous-type, and the replaced or deleted part of the chromosome was identified by so-called chromosome mapping. In addition to this kind of analysis at the chromosome level, non-LOH mutants were further characterized at the DNA sequence level to confirm that the mutation occurs in the *TK* gene or not. Recently we could establish the optimum condition for mutagenic radioadaptation in TK6 cells.[43] Under such condition as shown in Fig. 5, the greatest reduction in *TK* mutation frequency was observed in TK6 cells exposed to a challenging X-ray irradiation (2 Gy), and the TK^- mutants so obtained were analyzed by the LOH system.[43]

The TK^- mutation frequency (MF) obtained after the challenging X-ray (2 Gy) exposure, 18.3×10^{-6} was reduced to 11.4×10^{-6} (62% of the original level) by inducing the radioadaptation (50 mGy of pre-X-irradiation at 6 hr before the above challenging X-irradiation; Fig. 6). LOH analysis could classify the TK^- mutational events as non-LOH (mostly mutations in the *TK* gene), hemizygous LOH (deletion of chromosome) and homozygous LOH (homologous recombination [HR] between chromosomes), as mentioned above.[40–42] Non-LOH events are, in theory, classified as chromosomal alterations, but most of non-LOH mutants obtained in this experiment were confirmed to be small mutations in the *TK* gene by DNA base sequencing of mRNA obtained from the mutants.[43] The pre-irradiation decreased the frequencies of non-LOH events and homozygous LOH events to 27% and 60% of the original levels, respectively. The frequency of hemizygous LOH events, however, was not significantly altered by the pre-irradiation. Since LOH events are most likely the consequence of DSB repair, we tried to investigate the influence of priming X-ray irradiation on DSB repair efficiency under the optimum condition for radioadaptation.

The repair efficiency of DSB *via* NHEJ was hardly influenced by the pre-irradiation of 50 mGy X-rays (Table 3). On the other hand, a ~70% enhancement in HR repair of DSB was observed after this treatment. The enhanced activity of HR observed in this experiment could reflect the activity of error-free DSB repair, providing a reduction in genetic alterations at the chromosome level. In fact, we observed a ~60% reduction in the induction of homozygous LOH as mentioned above. The chromosome-mapping analysis demon-

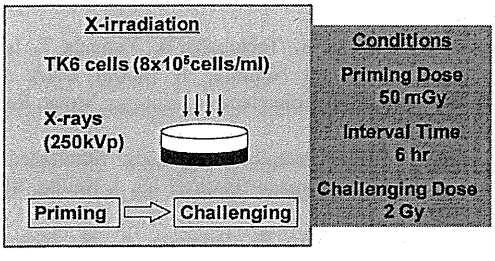

Fig. 5. An experimental scheme for mutagenic radioadaptation. The optimum conditions providing the greatest reduction in the frequency of *TK* mutations induced after a challenging X-ray (2 Gy) irradiation of TK6 cells, are shown in the right panel of this figure. The details have already been described in our previous work.[43]

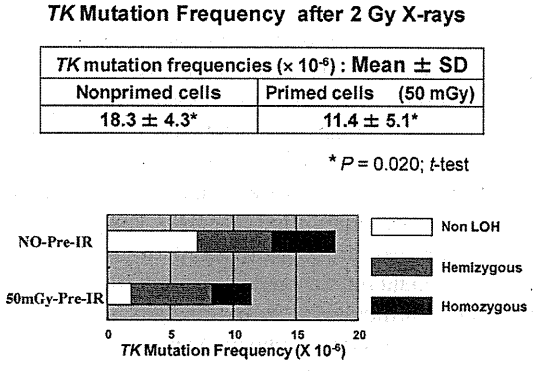

Fig. 6. Genetic analysis of radioadaptation induced by low-dose X-rays. Results of the *TK* mutation assay performed under the optimum condition for radioadaptation (Fig. 5) are summarized in the table, and the classification of the isolated TK^- mutants was made by LOH analysis and the results are shown in the histograms (see text).

Table 3. The effect of a priming X-ray exposure on DSB repair (X-ray - X-ray adaptive experiment).

a) NHEJ efficiency in TSCE5 cells

Exp.	Effect of IR (Relative MF*)
1	0.98
2	0.76
3	0.99
Average	0.91

*Relative MF was calculated as MF (X-rays + I-SceI)/MF (I-SceI).

b) HR efficiency in TSCER2 cells

Exp.	Effect of IR (Relative RF*)
1	2.2
2	1.2
3	1.7
Average	1.7

*Relative RF was calculated as RF (X-rays + I-SceI)/RF (I-SceI).

strated that the observed homozygous LOH events were mostly of the crossing-over type.[23] In contrast, the analysis of TK (+/–) revertants observed with our DSB repair assay suggests that HR in this I-SceI system mostly reflects a gene conversion activity, with a relatively small proportion of non-crossing-over events (data not shown). More supporting evidence is required to determine if an enhanced HR activity is reflected by the reduction in homozygous LOH events.

Further applications and perspectives

It is of theoretical and practical importance to estimate human health risks from low-doses of ionizing radiation. One example is the risk for astronauts exposed to space radiation, because the background radiation in space is, at least, more than 100-fold higher than the background level found on earth. Currently, we have the opportunity to study the influence of space radiation in TK6 cells, which were recently brought back to earth after preservation for more than four months, mostly in a frozen state, in the International Space Station. Assuming that the DNA damage caused by space radiation has been accumulated in the frozen cells, such damage could induce mutations when the cells begin to grow again. Furthermore, such damage might have the potential ability to induce radioadaptation and this radioadaptation might be detected as an enhancement in DSB repair in the I-SceI digestion system in the recovered cells.

The following points involved in our I-SceI digestion system merit discussion. Because our I-SceI system does not uncover all NHEJ and HR events, it is difficult to evaluate accurately the extent of DSB repair *via* both HR and NHEJ pathways. For example, our system does not monitor sister-chromatid HR, which is probably the major HR pathway in mammalian cells. Small gene conversion events, which do not extend into the exon 5 region, can also not be detected by this system. Although the I-SceI system may over-estimate the repair efficiency of NHEJ compared with HR, this methodology can still be considered to contribute to elucidating the DSB repair associated with low-dose IR exposure.

Finally, we would like to emphasize that the present evaluation of DSB repair using the I-SceI system, may contribute to our overall understanding of radioadaptation. Other types of studies regarding gene expression, epigenetic changes *etc.*, are also required for a more complete understanding.

ACKNOWLEDGMENTS

The authors greatly appreciate Professor Takeo Ohnishi of Nara Prefecture Medical University for providing us with the opportunity to present our work. They also appreciate Dr. Alasdair Gordon of Baylor College of Medicine in USA for preparing the manuscript of the present paper. This study was supported by the Budget for Nuclear Research of the Ministry of Education, Culture, Sports, Science and Technology, and was reviewed by the Atomic Energy Commission of Japan.

REFERENCES

1. Olivieri, G., Bodycote, Y. and Wolf. S. (1984) Adaptive response of human lymphocytes to low concentrations of radioactive thymidine. Science **223**: 594–597.
2. Wolf, S. (1996) Aspects of the adaptive response to very low doses of radiation and other agents. Mutat. Res. **358**: 135–142.
3. Wolf, S. (1998) The adaptive response in radiobiology: Evolving insights and implications. Environ. Health Perspect. **106**: 277–283.
4. Ikushima, T. (1987) Chromosomal response to ionizing radiation reminiscent of an adaptive response in cultured Chinese hamster cells. Mutat. Res. **180**: 215–221.
5. Sanderson, B. J. S. and Morely, A. A. (1986) Exposure of human lymphocytes to ionizing radiation reduces mutagenicity by subsequent radiation. Mutat. Res. **164**: 347–151.
6. Zhou, P. K., Liu, X. Y., Sun, W. Z., Zhang, Y. P. and Wei, K. (1993) Cultured mouse SR-1 cells exposed to low-dose of γ-rays become less susceptible to the induction of mutations by radiation as well as bleomycin. Mutagenesis **8**: 109–111.
7. Ueno, A. M., Vannais, D. B., Gustafson, S. L., Wong, J. C. and Waldren, C. A. (1996) A low adaptive dose of gamma-rays reduced the number and altered the spectrum of S1 mutants in human hamster hybrid cells. Mutat. Res. **358**: 161–169.
8. Wojewodska, M., Kruzewski, M., Iwanenko, K. and Szumiel, I. (1997) Effects of signal transduction in adapted lymphocytes: micronuclei frequency and DNA repair. Int. J. Radiat. Biol. **71**: 245–252.
9. Azzam, E. I., Raaphorst, G. P. and Mitchel, R. E. (1994) Radiation-induced adaptive response for protection against micronucleus formation and neoplastic transformation in C3H 10T1/2 mouse embryo cells. Radiat. Res. **138**: S28–S31.
10. Rigaud, O., Papadopoulo, D. and Moustacchi, E. (1993) Decreased deletion mutation in radioadapted human lymphoblast. Radiat. Res. **133**: 94–101.
11. Rigaud, O. and Moustacchi, E. (1996) Radioadaptation for gene mutation and the possible molecular mechanisms of the adaptive response. Mutat. Res. **358**: 127–134.
12. Zhou, P.-K. and Rigaud, O. (2001) Down-regulation of the human *CDC16* gene after exposure to ionizing radiation: A possible role in the radioadaptive response. Radiat. Res. **155**: 43–49.
13. Sasaki, M. S., Ejima, Y., Tachibana, A., Yamada, T., Ishizaki, K., Shimizu, T. and Nomura, T. (2002) DNA damage response pathway in radioadaptive response. Mutat. Res. **504**: 101–118.
14. Szumiel, I. (2005) Adaptive responses: Stimulated DNA repair or decreased damage fixation? Int. J. Radiat. Biol. **81**: 233–241.
15. Coleman, M. A., Yin, E., Peterson, L. E., Nelson, D., Sorensen, K., Tucker, J. D. and Wyrobeck, A. J. (2005) Low-dose irradiation alters the transcript profiles of human lymphoblastoid cells inducing genes associated with radioadaptive response. Radiat. Res. **164**: 369–382.
16. Swant, S. G., Randers-Pehrson, G., Metting, N. F. and Hall,

E. J. (2001) Adaptive response and the bystander effect induced by radiation in C3H 10T1/2 cells in culture. Radiat. Res. **156**: 177–180.
17. Zhou, H. N., Randers-Pehrson, G., Geard, C. R., Brenner, D. J., Hall, E. J. and Hei, T. K. (2003) Interaction between radiation-induced adaptive response and bystander mutagenesis in mammalian cells. Radiat. Res. **160**: 512–516.
18. Bonner, W. M. (2003) Thresholds, bystander effect, and adaptive response. Proc. Natl. Acad. Sci. USA, **100**: 4973–4975.
19. Mitchell, S. A., Marino, S. A., Brenner, D. J. and Hall, E. J. (2004) Bystander effect and adaptive response in C3H 10T (1/2) cells. Int. J. Radiat. Biol. **80**: 465–472.
20. Hei, T. K., Persaud, R., Zhou, H. and Suzuki, M. (2004) Genotoxicity in the eyes of bystander cells. Mutat. Res. **568**: 111–120.
21. Matsumoto, H., Hamada, N., Takahashi, A., Kobayashi, Y. and Ohnishi, T. (2007) Vanguards of paradigm shift in radiation biology: radiation-induced adaptive and bystander responses. J. Radiat. Res. **48**: 97–106.
22. Iyer, R. and Lehnert, B. E. (2002) Low-dose, low-LET ionizing radiation-induced radioadaptation and associated early responses in unirradiated cells. Mutation Res. **503**: 1–9.
23. Matsumoto, H., Takahashi, A. and Ohnishi, T. (2004) Radiation-induced adaptive and bystander effects. Biol. Sci. Space **18**: 247–254.
24. McLaughlin, L. M. and Demple, B. (2005) Nitric oxide-induced apoptosis in lymphoblastoid and fibroblast cells dependent on the phosphorylation and activation of p53. Cancer Res. **65**: 6097–6104.
25. Shimizu, T., Kato, T. Jr., Tachibana, A. and Sasaki, M. S. (1999) Coordinated regulation of radioadaptive response by protein kinase C and p38 nitrogen-activated protein kinase. Exp. Cell. Res., **251**: 424–432.
26. Otsuka, K., Koana, T., Tauchi, H. and Sakai, K. (2006) Activation of antioxidative enzymes induced by low-dose-rate whole body γ irradiation: adaptive response in terms of initial DNA damage. Radiat. Res. **166**: 474–478.
27. Inoue, M., Shen, G-P., Chaudhry, M. A., Galick, H., Blaisdell, J. O. and Wallace, S. S. (2004) Expression of the oxidative base excision repair enzymes is not induced in TK6 human lymphoblastoid cells after low doses of ionizing radiation. Radiat. Res. **161**: 409–417.
28. Yongblom, J. H., Wiencke, J. K. and Wolf, S. (1989) Inhibition of the adaptive response of human lymphocytes to very low doses of ionizing radiation by the protein synthesis inhibitor cycloheximide. Mutat. Res. **227**: 257–261.
29. Wang, H. P., Long, X. H., Sun, Z. Z., Rigaud, O., Xu, Q. Z., Huang, Y. C., Sui, J. L., Bai, B. and Zhou, P. K. (2006) Identification of differentially transcribed genes in human lymphoblastoid cells irradiated with 0.5 Gy of γ-ray and the involvement of low dose radiation inducible CHD6 gene in cell proliferation and radiosensitivity. Int. J. Radiat. Biol. **82**: 181–190.
30. Ding, L.-H., Shingyoji, M., Chen, F., Hwang, J.-J., Burma, S., Lee, C., Chen, J.-F. and Chen, D. J. (2005) Gene expression profiles of normal human fibroblasts after exposure to ionizing radiation: a comparative study of low and high doses. Radiat. Res. **164**: 17–26.
31. Taki, K., Wang, B., Nakajima, T., Wu, J., Ono, T., Uehara, Y., Matsumoto, T., Oghiso, Y., Tanaka, K., Ichinohe, K., Nakamura, S., Tanaka, S., Magae, J., Kakimoto, A. and Nenoi, M. (2009) Microarray analysis of differentially expressed genes in the kidneys and testes of mice after long-term irradiation with low-dose-rate γ-rays. J. Radiat. Res. **50**: 241–252.
32. Jackson, S. P. (2002) Sensing and repairing DNA double-strand breaks. Carcinogenesis **23**: 687–696.
33. Valerie, K. and Povirk, L. F. (2003) Regulation and mechanisms of mammalian double-strand break repair. Oncogene **22**: 5792–5812.
34. Cramers, P., Atanasova, P., Vrolijk, H., Darroudi, F., van Zeeland, A. A., Huiskamp, R., Mullenders, L. H. F., Kleinjans and Jos, C. S. (2005) Pre-exposure to low-doses: modulation of X-ray-induced DNA damage and repair? Radiat. Res. **164**: 383–390.
35. Ikushima, T., Aritomi, H. and Morisita, J. (1996) Radioadaptive response: efficient repair of radiation- induced DNA damage in adapted cells. Mutat. Res. **358**: 193–198.
36. Honma, M., Izumi, M., Sakuraba, M., Tadokoro, S., Sakamoto, H. Wang, W., Yatagai, F. and Hayashi, M. (2003) Deletion, rearrangement, and gene conversion; genetic consequences of chromosomal double-strand breaks in human cells. Environ. Mol. Mutagen **42**: 288–298.
37. Honma, M., Sakuraba, M., Koizumi, T., Takashima, T., Sakamoto, H. and Hayashi, M. (2007) Non-homologous end-joining for repairing I-SceI induced DNA double strand breaks in human cells. DNA Repair **6**: 781–788.
38. Yatagai, F., Suzuki, M., Ishioka, N., Ohmori, H. and Honma. M. (2008) Repair of I-SceI Induced DSB at a specific site of chromosome in human cells: influence of low-dose, low-dose rate gamma-rays. Radiat. Environ. Biophys. **47**: 439–444.
39. Pastwa, E. and Blasiak, J. (2003) Non-homologous end-joining. Acta Biochem. Pol. **50**: 891–908.
40. Morimoto, S., Kato, T., Honma, M., Hayashi, M., Hanaoka, F. and Yatagai, F. (2002) Detection of genetic alterations induced by low-dose X rays: analysis of loss of heterozygosity for *TK* mutation in human lymphoblastoid cells. Radiat. Res. **157**: 533–538.
41. Morimoto, S., Honma, M. and Yatagai, F. (2002) Sensitive detection of LOH events in a human cell line after C-ion beam exposure. J. Radiat. Res. **43** (Suppl.): S163–S167.
42. Umebayashi, Y., Honma, M., Abe, T., Ryuto, H., Suzuki, H., Shimazu, T., Ishioka, N., Iwaki, M. and Yatagai, F. (2005) Mutation induction after low-dose carbon-ion beam irradiation of frozen human cultured cells. Biol. Sci. Space **19**: 237–241.
43. Yatagai, F., Umebayashi, Y., Honma, M., Sugasawa, K., Takayama, Y. and Hanaoka, F. (2008) Mutagenic radioadaptation in a human lymphoblastoid cell line. Mutat. Res. **638**: 48–55.

Received on April 27, 2009
Revision received on July 1, 2009
Accepted on July 13, 2009
J-STAGE Advance Publication Date: August 13, 2009

Genes and Environment, Vol. 32, No. 1 pp. 7–13 (2010)

Regular article

Mutagenicity of Heterocyclic Amines by Biomimetic Chemical Models for Cytochrome P450 in Ames Assay

Keiko Inami[1,2], Minako Nagao[1,3], Satoko Ishikawa[1,3] and Masataka Mochizuki[1,2]

[1]Kyoritsu University of Pharmacy, Tokyo, Japan
[2]Faculty of Pharmaceutical Sciences, Tokyo University of Science, Chiba, Japan
[3]Faculty of Pharmacy, Keio University, Tokyo, Japan

(Received December 26, 2009; Revised January 25, 2010; Accepted January 26, 2010)

Heterocyclic amines (HCAs) are a family of mutagenic and carcinogenic compounds produced during cooking or other burning processes, and exist in the environment. HCAs are metabolically activated by cytochrome P450, conjugated by phase II enzymes, to react with guanine bases. The aim of this study is to establish a chemical model for cytochrome P450 as an alternative to S-9 mix for detecting HCA mutagenicity in Salmonella strain. A chemical model was developed by comparing the mutagenicity of 3-amino-1-methyl-5H-pyrido[4,3-b]indole (Trp-P-2) in the presence of an iron porphyrin and an oxidant. The iron porphyrin derivatives, water-soluble 5,10,15,20-tetrakis(1-methylpyridinium-4-yl)porphyrinatoiron (III) chloride (4-MPy) or water-insoluble 5,10,15,20-tetrakis (pentafluorophenyl)porphyrinatoiron (III) chloride (F_5P), and the oxidant tert-butyl hydroperoxide (t-BuOOH), magnesium monoperoxyphthalate or iodosylbenzene were used. 4-MPy or F_5P with t-BuOOH activated Trp-P-2, and the activity was similar with either porphyrin. Water-soluble model has a better chance to detect unstable compound, since the tester strain was exposed in the whole incubation period in the mutation procedure with 4-MPy. The effectiveness of 4-MPy/t-BuOOH was evaluated with other HCAs; IQ, MeIQ, MeIQx, Glu-P-1, Glu-P-2, PhIP, Trp-P-1, MeAαC and AαC. All HCAs except for MeAαC and AαC were mutagenic in Salmonella typhimurium TA1538. MeAαC and AαC were not mutagenic in TA1538, but they were mutagenic in S. typhimurium TA1538/pYG219, which overexpresses O-acetyltranferase on the TA1538 genetic background. Although the HCAs mutagenicity with the chemical model was weaker than that with S-9 mix, the chemical models activated HCAs without S-9 mix in the Ames assay.

Key words: iron porphyrin, chemical model, cytochrome P450, metabolic activation, heterocyclic amine

Introduction

Heterocyclic amines (HCAs) are found in broiled, fried or barbecued meats and other proteinaceous foods, as well as in tobacco smoke (1–6). The consumption or intake of HCAs is suspected to be correlated with the induction of cancers (7–13). HCAs are a family of mutagenic and carcinogenic compounds produced during the pyrolysis of creatine, amino acids and glucose. HCAs are classified into two groups based on structure: 2-amino-3-methylimidazo[4,5-*f*]quinoline (IQ)-type and non-IQ type. IQ-type comprises HCAs that are characterized by a 2-aminoimidazole structure, while non-IQ type is typically characterized by a 2-aminopyridine structure (14–16) (Fig. 1).

The HCAs are oxidized to *N*-hydroxyamines by cytochrome P450 (17–20), and then conjugated by acetylation, sulfation and proline conjugation, and finally activated to react with guanines (21–25). The HCAs are known to be activated also by prostaglandin H synthase, however, the activation mechanism is not known (26).

Rat S-9 mix is useful in obtaining reliable data when used for activation in the Ames assay, since the S-9 mix includes many kinds of cytochrome P450 containing iron (Fe) porphyrin active sites capable of metabolizing a large number of chemicals to reactive forms (27,28). However the S-9 mix has difficulty maintaining constant enzymatic activity (29). In order to overcome the difficulty, an alternate *in vitro* model for cytochrome P450, consisting of a Fe porphyrin and an oxidant was applied in the Ames mutation assay. This model may be used as an alternative to animals in primary screening. The chemical model has been used previously for detecting the mutagenicity of polyaromatic hydrocarbons (30,31), aromatic amines and amides in the Ames assay (31,32). In this study, a chemical model which combined a Fe porphyrin with an oxidant was developed to detect the mutagenicity of HCAs. The Fe porphyrins, water-soluble 5,10,15,20-tetrakis(1-methylpyridinium-4-yl)

[4]Correspondence to: Keiko Inami, Faculty of Pharmaceutical Sciences, Tokyo University of Science, Yamazaki 2641, Noda, Chiba 278-8510, Japan. Tel/Fax: +81-4-7121-3641, E-mail: inami@rs.noda.tus.ac.jp

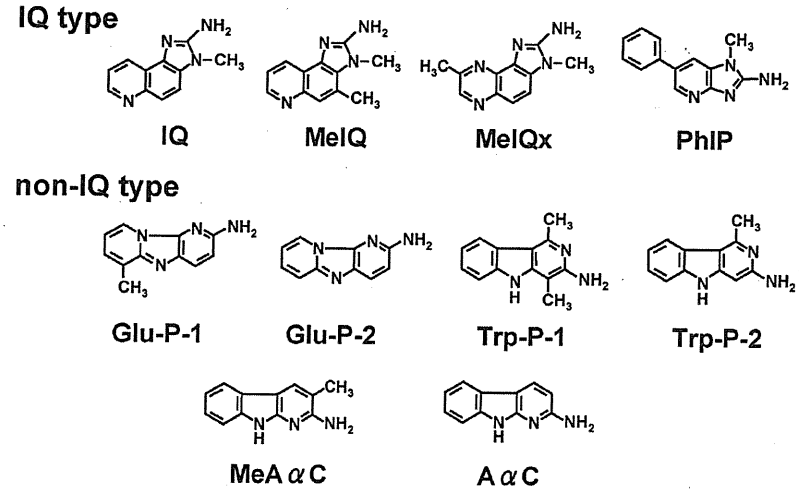

Fig. 1. Structure of HCAs.

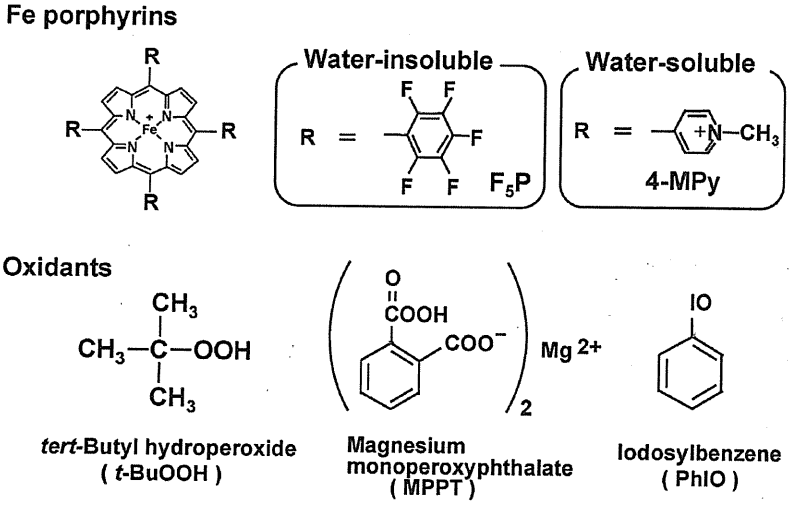

Fig. 2. Structure of chemical models Fe porphyrins and peroxides used.

porphyrinatoiron(III) chloride (4-MPy) or water-insoluble 5,10,15,20-tetrakis(pentafluorophenyl)porphyrinatoiron(III) chloride (F_5P) was used, and as oxidants, *tert*-butyl hydroperoxide (*t*-BuOOH), magnesium monoperoxyphthalate (MPPT) or iodosylbenzene (PhIO) was used. The reaction conditions were optimized by comparing the mutagenic activity of 3-amino-1-methyl-5*H*-pyrido[4,3-*b*]indole (Trp-P-2) in *S. typhimurium* TA1538, and the effectiveness of 4-MPy/*t*-BuOOH with other HCAs using the Ames assay was then evaluated.

Materials and Methods

Chemicals: *t*-BuOOH, F_5P and MPPT were purchased from Sigma-Aldrich Corp. (St. Louis, USA). Sodium ammonium hydrogenphosphate tetrahydrate was purchased from Merck (Darmstadt, Germany). Tetrakis (1-methylpyridinium-4-yl)porphine *p*-toluenesulfonate and PhIO were purchased from Tokyo Chemical Industry Co., Ltd (Tokyo, Japan). Bacto agar and bacto nutrient broth were obtained from Becton Dickinson Microbiology Systems (Sparks, USA). Other reagents used were purchased from Wako Pure Chemical Industries (Osaka, Japan). 4-MPy was synthesized as described (33). The purity of 4-MPy was determined by ultraviolet spectroscopy. 3-Amino-1,4-dimethyl-5*H*-pyrido[4,3-*b*]indole (Trp-P-1) acetate and Trp-P-2 acetate were recrystallized from ethanol and ethyl acetate before use. The structure of the chemical models used is shown in Fig. 2.

Mutation assay using the chemical model: The mutation assay was based on the Ames test (34,27),

utilizing a chemical model consisting of Fe(III) porphyrin and an oxidant as a substitute for the metabolic activation system. Professor B. N. Ames (University of California, Berkeley, USA) provided the *S. typhimurium* TA1538, and Dr. T. Nohmi (National Institute of Health Sciences, Tokyo, Japan) provided the *S. typhimurium* TA1538/pYG219. 4-MPy (50 nmol/20 μL), *t*-BuOOH (150 nmol/20 μL) and MPPT (50 nmol/20 μL) were dissolved in 0.1 M sodium phosphate buffer (pH 7.4), and PhIO (250 nmol/20 μL) was dissolved in methanol. F_5P (50 nmol/20 μL), 2-amino-3,8-dimethylimidazo[4,5-*f*]quinoxaline (MeIQx), 2-amino-1-methyl-6-phenylimidazo[4,5-*b*]pyridine (PhIP) hydrochloride, 2-amino-3-methyl-9*H*-pyrido[2,3-*b*]indole (MeAαC) and 2-amino-9*H*-pyrido[2,3-*b*]indole (AαC) were dissolved in acetonitrile, and 2-amino-3-methylimidazo[4,5-*f*]quinoline (IQ), 2-amino-3,4-dimethylimidazo[4,5-*f*]quinoline (MeIQ), Trp-P-1 acetate, 2-amino-6-methyldipyrido[1,2-α:3′,2′-*d*]imidazole (Glu-P-1) hydrochloride and 2-aminodipyrido[1,2-α:3′,2′-*d*]imidazole (Glu-P-2) hydrochloride were dissolved in H_2O. Trp-P-2 acetate was dissolved in *N*,*N*-dimethylformamide when water-insoluble F_5P was used, whereas it was dissolved in H_2O when water-soluble 4-MPy was used. All mutagens showed no mutagenicity in the absence of the chemical model system in Salmonella strains.

Preincubation assay using water-soluble chemical activation system (35): An aliquot of the water-soluble 4-MPy (20 μL) and mutagen (20 μL), both in solutions, were mixed, and oxidant (20 μL), 0.1 M sodium phosphate buffer (pH 7.4, 0.5 mL), and a culture of the tester strains (0.1 mL) were added. The mixture was then incubated for 10 sec, 1, 3, 5, 10, or 20 min at 25°C with shaking (120 strokes/min), and top agar (2 mL) was added. The mixture was then poured onto a minimal-glucose agar plate. After incubation for 44 h at 37°C, colonies were counted using a colony analyzer (System Science Co. Ltd., Tokyo, Japan). Mutagenic activity was tested at whole incubation periods, however, the highest mutagenic activity was observed at a different incubation period for each chemical model (31). In this study, the optimal incubation period for each of the assay conditions was selected for data presentation. The results were considered positive if the assay produced reproducible, dose-related increases in the number of revertants.

Preincubation for water-insoluble chemical activation and direct mutagenicity assay (35): An aliquot of the water-insoluble F_5P (20 μL) and mutagen (20 μL) in solution were mixed, and oxidant (20 μL) in a solution was added. The mixture was then incubated for 1, 3, 5, 10 or 20 min at 25°C with shaking (120 strokes/min), and 0.1 M sodium phosphate buffer (pH 7.4, 0.5 mL), a culture of tester strain (0.1 mL), and top agar (2 mL) were added. The mixture was then poured onto a minimal-glucose agar plate. After incubation for 44 h at 37°C, colonies were counted. The data are presented as described previously.

Results

Optimization of model for detecting HCAs mutagenicity in the Ames assay: The most efficient chemical model for detecting the HCAs mutagenicity was developed by comparing Trp-P-2 mutagenicity, consisting of a Fe porphyrin, water-soluble 4-MPy or water-insoluble F_5P plus *t*-BuOOH. The assay protocols using the chemical models were already reported (35). The chemical model containing a water-soluble porphyrin was suitable for addition of a tester strain during incubation, whereas the F_5P chemical model was suitable for adding a tester strain after incubation.

Trp-P-2 in the presence of each chemical model showed the highest mutagenicity at the 20 min reaction time using each procedure (Fig. 3). The mutagenicity of Trp-P-2 was similar with either 4-MPy or F_5P, in the presence of *t*-BuOOH (Fig. 4). Water-soluble 4-MPy has been shown to detect unstable intermediates formed in the reaction mixture therefore we used preincubation method where the tester strain was added over incubation periods (32).

The models were composed of water-soluble 4-MPy, and an oxidant-*t*-BuOOH, MPPT or PhIO, and were used as alternatives for S-9 mix. One dose of the porphyrin (50 nmol/plate) was used since the mutagenicity of polyaromatic hydrocarbons, aromatic amines and amides have been successfully detected in the presence of 50 nmol/plate of the porphyrin (30,32). The concentration of the oxidants was determined as those not

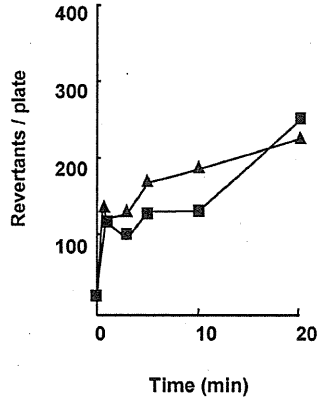

Fig. 3. Effect of incubation period on Trp-P-2 mutagenicity in *S. typhimurium* TA1538. Preincubation assay involved exposing a tester strain with reaction mixture using water-soluble 4-MPy (▲) or adding a tester strain into a reaction mixture after the incubation period using water-insoluble F_5P (■). The concentration of Trp-P-2 was 25 nmol/plate.

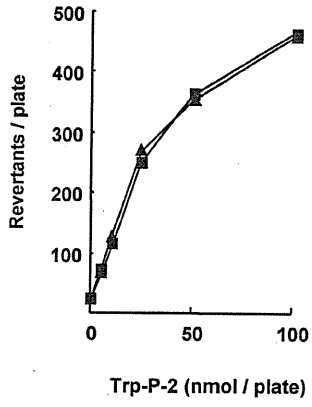

Fig. 4. Effect of Fe porphyrin on Trp-P-2 activation in *S. typhimurium* TA1538 in the presence of a Fe porphyrin plus *t*-BuOOH. Preincubation assay involves exposing a tester strain with reaction mixture using water-soluble 4-MPy (▲) or adding a tester strain into a reaction mixture after the incubation period using water-insoluble F_5P (■).

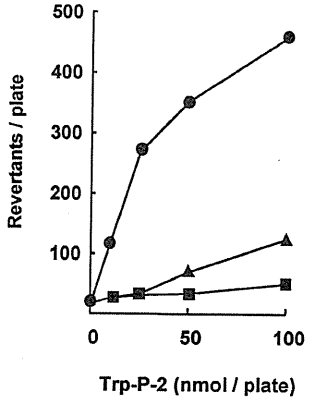

Fig. 5. Effect of oxidants on Trp-P-2 activation in *S. typhimurium* TA1538 in the presence of 4-MPy. *t*-BuOOH (●), MPPT (■) or PhIO (▲) preincubated with 4-MPy in 0.1 M phosphate buffer for 20 min.

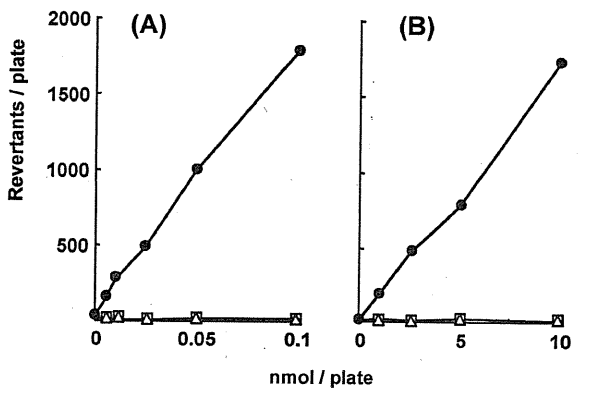

Fig. 6. Mutagenicity of IQ (A) and Glu-P-1 (B) in *S. typhimurium* TA1538 in the presence of 4-MPy/*t*-BuOOH. Complete system contained mutagen in water, 4-MPy and *t*-BuOOH in sodium phosphate buffer (pH 7.4) and incubated for 20 min (●). The control system comprised without 4-MPy (□), without *t*-BuOOH (△), and mutagen alone (○), which all overlapped.

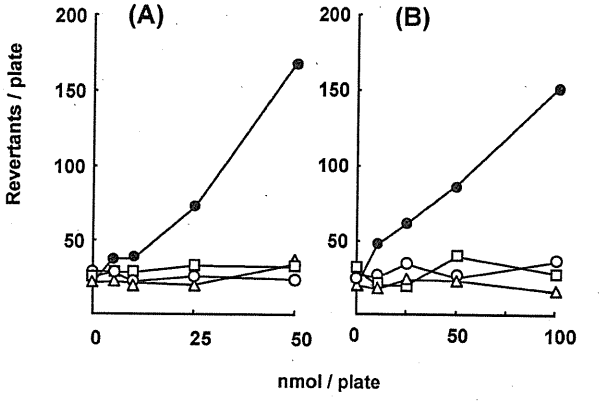

Fig. 7. Mutagenicity of MeAαC (A) and AαC (B) in *S. typhimurium* TA1538/pYG219 in the presence of 4-MPy/*t*-BuOOH. Complete system contained a mutagen in acetonitrile, 4-MPy and *t*-BuOOH in sodium phosphate buffer (pH 7.4) preincubated for 10 sec (●). The control system comprised without 4-MPy (□), without *t*-BuOOH (△), and mutagen alone (○).

showing cytotoxicity, and then the ratio of the porphyrin and the oxidant is different among each oxidant. Trp-P-2 mutagenicity in the presence of the various chemicals was compared (Fig. 5).

The activation capacity was in the order: *t*-BuOOH > MPPT > PhIO. The results showed that the 4-MPy/*t*-BuOOH was the most effective chemical model to detect HCAs mutagenicity.

Detection of HCAs mutagenicity in the presence of 4-MPy/t-BuOOH: Activation of ten HCAs; IQ, MeIQ, MeIQx, Glu-P-1, Glu-P-2, PhIP, Trp-P-1, Trp-P-2, MeAαC, AαC, in the presence of 4-MPy/*t*-BuOOH was evaluated in the Salmonella strains. Figure 6 shows the metabolic activation of IQ and Glu-P-1, which are representative of an IQ-type and a non-IQ type HCA, respectively. All IQ type HCAs (IQ, MeIQ, MeIQx, PhIP) and non-IQ type HCAs (Glu-P-1, Glu-P-2, Trp-P-1) were mutagenic in *S. typhimurium* TA1538 in the presence of 4MPy/*t*-BuOOH with 20 min preincubation. MeAαC and AαC were not mutagenic in the *S. typhimurium* TA1538 strain. When *S. typhimurium* TA1538/pYG219 (36), overexpressing *O*-acetyltransferase on the genetic background of the *S. typhimurium* TA1538, was used for detecting mutagenicity of MeAαC and AαC (Fig. 7), both were mutagenic in a dose-dependent manner in the presence of 4-MPy/*t*-BuOOH.

The mutagenic activity was determined from the slopes of dose-revertants profile in the initial linear part of the profile by the least squares method (Table 1). The

Table 1. Relative mutagenicity of HCAs in the presence of 4-MPy/*t*-BuOOH in *S. typhimurium* TA1538

HCAs	Revertants/nmol
IQ	17444±43.4
MeIQ	5284±41.0
MeIQx	4510±16.1
Glu-P-1	169±51.2
Glu-P-2	29±14.3
PhIP	48±47.2
Trp-P-2	10± 2.7
Trp-P-1	7±10.4
MeAαC*	3±11.7
AαC*	1± 3.1

**S. typhimurium* TA1538/pYG219.

study with S-9 mix used *S. typhimurium* TA98 carrying plasmid pKM101, which has higher sensitivity for DNA damage due to SOS repair response (37,38). On the contrary, *S. typhimurium* TA1538 and TA1538/pYG219 were used for detecting the HCAs mutagenicity in the chemical model since, specifically, frame-shift type mutation was detected. Since mutagenicity of some HCAs (IQ, MeIQ, MeIQx, PhIP) with S-9 mix has been reported to be the same in between *S. typhimurium* TA 1538 and TA98, the mutagenic activity using the chemical model was compared with the activity using S-9 mix (39).

The activity with the chemical model was smaller by two orders of magnitude than that with S-9 mix. However, IQ-type HCAs mutagenicity was higher than that of non-IQ type HCAs in both activating systems. Thus, the HCAs mutagenicity with 4-MPy/*t*-BuOOH was similar in tendency with that of S-9 mix.

Discussion

The chemical model as an alternative for S-9 mix has been studied for application in the Ames assay. The F_5P/MPPT and 4-MPy/*t*-BuOOH activate promutagenic polyaromatic hydrocarbons (30,31), aromatic amines and amides (31,32), respectively, to be mutagenic in Salmonella strains. In this study, we developed the test conditions for detecting mutagenicity of Trp-P-2 in the Ames assay and then ten HCAs were evaluated their mutagenicity in *S. typhimurium*.

Application of the chemical model in the Ames assay has been reported by Salmeen *et al.* and Rueff *et al* (40,41). In their procedures, the extract of the reaction mixture was used for detecting the mutagenicity. On the contrary, we added a bacteria strain to the reaction mixture directly (35). The procedure we developed has the advantage of simplifying the handling. In the mutation procedure with water-soluble 4-MPy/*t*-BuOOH where the bacterial strain coexisted during an incubation period, the mutagenicity of 2-acetylaminofluorene was caused by *N*-hydroxyacetylamino compounds (32). Whereas in the procedure with water-insoluble F_5P/*t*-BuOOH where the bacterial culture was added to the reaction mixture after an incubation period, and the mutagenicity of 2-acetylaminofluorene was due to 2-nitro-9-fluorenone (42). The results showed that the preincubation method using the 4-MPy/*t*-BuOOH has a better chance to detect unstable intermediates.

As regards an apparent superiority of the oxidants for activation of mutagens, Rueff *et al.* reported that aromatic amines (2-aminofluorene, 2-acetylaminofluorene) and HCAs (IQ) became more mutagenic with alkylhydroperoxide than that with peroxy acid or PhIO (41). In this study, *t*-BuOOH plus Fe porphyrin activated HCAs. Polyaromatic hydrocarbons in the presence of Fe porphyrin are mutagenic with peroxy acid (30,31), while aromatic amines are mutagenic with *t*-BuOOH (31,32). The oxidant specificity for the activation of mutagens is the same as that reported by Rueff *et al* (41). It has been reported that a different active species was formed by alkylhydroperoxide and peroxy acid in the presence of Fe porphyrin (43). In general, peroxy acid or PhIO formed an oxoiron (IV) porphyrin π cation radical, whereas alkylhydroperoxide generated alkoxyl radical by a Fenton type reaction. The specificity of the oxidant in a chemical model for activating mutagens might be due to the different active species in the high valent Fe-O complex formed.

The mutagenicity of HCAs activated with the chemical model was lower than that with the S-9 mix (38), probably because of a lack of phase II enzymes in the chemical models. MeAαC and AαC in the presence of 4-MPy/*t*-BuOOH were not mutagenic in *S. typhimurium* TA1538, however, they were mutagenic in *S. typhimurium* TA1538/pYG219, which overexpresses phase II enzyme *O*-acetyltransferase (36). These results suggest that the phase II enzyme is a key factor in the activation of HCAs. Since HCAs have almost the same mutagenic activity in *S. typhimurium* TA1538 and in *S. typhimurium* TA98 (39), *S. typhimurium* TA1538 was used in this study. The mutagenic potential with 4-MPy/*t*-BuOOH in *S. typhimurium* TA1538 was smaller by two orders of magnitude than that with S-9 mix in *S. typhimurium* TA98, however, the mutagenic strength on the basis of mutagen structure was similar in order in both the S-9 mix and the chemical model. 4-MPy/*t*-BuOOH apparently activated HCAs to mutagenic species in the present investigation.

In conclusion, the metalloporphyrin/oxidant system for cytochrome P450 as a biomimetic system for S-9 mix could be used for detecting promutagenic heterocyclic amines without using an enzymatic activating system in the primary screening assay for DNA damaging agents.

Acknowledgements: We thank Dr. T. Nohmi, Nation-

al Institute of Health Sciences, for providing the *S. typhimurium* TA1538/pYG219 strain. This work was supported in part by a Grant-in-Aid from the Ministry of Education, Culture, Sports, Science and Technology of Japan and by a Grant-in-Aid for the Science Research Promotion Fund from the Japan Private School Promotion Foundation.

References

1 Sugimura T. Studies on environmental chemical carcinogenesis in Japan. Science. 1986; 233: 312–18.
2 Sugimura T. Overview of carcinogenic heterocyclic amines. Mutat Res. 1997; 376: 211–19.
3 Sugimura T, Kawachi T, Nagao M, Yahagi T, Seino Y, Okamoto T, Shudo K, Kosuge T, Tsuji K, Wakabayashi K, Iitaka Y, Itai A. Mutagenic principle(s) in tryptophan and phenylalanine pyrolysis products. Proc Jpn Acad. 1977; 53: 58–61.
4 Yamamoto T, Tsuji K, Kosuge T, Okamoto T, Shudo K, Takeda K, Iitaka Y, Yamaguchi K, Seino Y, Yahagi T, Nagao M, Sugimura T. Isolation and structure determination of mutagenic substances in L-glutamic acid pyrolysate. Proc Jpn Acad. 1978; 54: 248–50.
5 Wakabayashi K, Ushijima H, Takahashi M, Nukaya H, Kim S-B, Hirose M, Ochiai M, Sugimura T, Nagao M. Exposure to heterocyclic amines. Environ Health Perspect. 1993; 99: 129–33.
6 Sinha R, Rothman N, Salmon CP, Knize MG, Brown ED, Swanson CA, Rhodes D, Rossi S, Felton JS, Levander OA. Heterocyclic amine content in beef cooked by different methods to varying degrees of doneness and gravy made from meat drippings. Food Chem Toxicol. 1998; 36: 279–87.
7 Norell SE, Ahlom A, Erwald R, Jacobson G, Lindberg-Navier I, Olin R, Törnberg B, Wiechel K. Diet and pancreatic cancer: a case-control study. Am J Epidemiol. 1986; 124: 894–902.
8 Steineck G, Hagman U, Gerhardsson M, Norell SE. Vitamin A supplements, fried foods, fat and urothelial cancer. A case-referent study in Stockholm in 1985–87. Int J Cancer. 1990; 45: 1006–11.
9 Schiffman MH, Felton JS. Fried foods and the risk of colon cancer. Am J Epidemiol. 1990; 131: 376–8.
10 Gerhardsson de Verdier M, Hagman U, Peters RK, Steineck G, Övervik E. Meat, cooking methods and colorectal cancer: a case-referent study in Stockholm. Int J Cancer. 1991; 49: 520–5.
11 Ikeda M, Yoshimoto K, Yoshimura T, Kono S, Kato H, Kuratsune M. A cohort study on the possible association between broiled fish intake and cancer. Gann. 1983; 74: 640–8.
12 Santarelli RL, Pierr F, Corpet DE. Proposed meat and colorectal cancer: a review of epidemiologic and experimental evidence. Nutr Cancer. 2008; 60: 131–44.
13 Alaejos MS, González V, Afonso AM. Exposure to heterocyclic aromatic amines from the consumption of cooked red meat and its effect on human cancer risk: a review. Food Addit Contam Part A Chem Anal Control Expo Risk Assess. 2008; 25: 2–24.
14 Tsuda M, Negishi C, Makino R, Sato S, Yamaizumi Z, Hirayama T, Sugimura T. Use of nitrite and hypochlorite treatments in determination of contributions of IQ-type and non-IQ-type heterocyclic amines to the mutagenicities in crude pyrolyzed materials. Mutat Res. 1985; 147: 335–41.
15 Jägerstad M, Olsson K, Glivas S, Negishi C, Wakabayashi K, Tsuda M, Sato S, Sugimura T. Formation of 2-amino-3,8-dimethylimidazo-[4,5-*f*]quinoxaline in a model system by heating creatinine, glycine and glucose. Mutat Res. 1984; 126: 239–44.
16 Shioya M, Wakabayashi K, Sato S, Nagao M, Sugimura T. Formation of a mutagen, 2-amino-1-methyl-6-phenylimidazo[4,5-*b*]pyridine (PhIP) in cooked beef, by heating a mixture containing creatinine, phenylalanine and glucose. Mutat Res. 1987; 191: 133–8.
17 Ishii K, Ando M, Kamataki T, Kato R, Nagao M. Metabolic activation of mutagenic tryptophan pyrolysis products (Trp-P-1 and Trp-P-2) by a purified cytochrome P-450-dependent monooxygenase system. Cancer Lett. 1980; 9: 271–6.
18 Mita S, Ishii K, Yamazoe Y, Kamataki T, Kato R, Sugimura T. Evidence for the involvement of *N*-hydroxylation of 3-amino-1-methyl-5*H*-pyrido[4,3-*b*]indole by cytochrome P450 in the covalent binding to DNA. Cancer Res. 1981; 41: 3610–14.
19 Snyderwine EG, Schut HAJ, Adamson RH, Thorgeirsson UP, Thorgeirsson SS. Metabolic activation and genotoxicity of heterocyclic arylamines. Cancer Res. 1992; 52: 2099s–2102s.
20 Turesky RJ, Guengerich FP, Guillouzo A, Langouët S. Metabolism of heterocyclic aromatic amines by human hepatocytes and cytochrome P4501A2. Mutat Res. 2002; 506–507: 187–95.
21 Hashimoto Y, Shudo K, Okamoto T. Metabolic activation of a mutagen, 2-amino-6-methyldipyrido[1, 2-*a*: 3′,2′-*d*]imidazole. Identification of 2-hydroxyamino-6-methyldipyrido[1,2-*a*: 3′,2′-*d*]imidazole and its reaction with DNA. Biochem Biophys Res Commun. 1980; 92: 971–6.
22 Hashimoto Y, Shudo K, Okamoto T. Activation of a mutagen, 3-amino-1-methyl-5*H*-pyrido[4,3-*b*]indole. Identification of 3-hydroxyamino-1-methyl-5*H*-pyrido[4,3-*b*]indole and its reaction with DNA. Biochem Biophys Res Commun. 1980; 96: 355–62.
23 Snyderwine EG, Roller PP, Adamson RH, Sato S, Thorgeirsson SS. Reaction of *N*-hydroxylamine and *N*-acetoxy derivatives of 2-amino-3-methylimidazo[4,5-*f*]quinoline with DNA. Synthesis and identification of *N*-(deoxyguanosin-8-yl)-IQ. Carcinogenesis. 1988; 9: 1061–5.
24 Ochiai M, Nagaoka H, Wakabayashi K, Tanaka Y, Kim S-B, Tada A, Nukaya H, Sugimura T, Nagao M. Identification of N^2-(deoxyguanosin-8-yl)-2-amino-3,8-dimethylimidazo[4,5-*f*]quinoxaline 3′,5′-diphosphate, a major DNA adduct, detected by nuclease P1 modification of ^{32}P-postlabeling method, in the liver of rats fed MeIQx. Carcinogenesis. 1993; 14: 2165–70.
25 Schut HAL, Snyderwine EG. DNA adducts of heterocyclic amine food mutagens: implications for mutagenesis

and carcinogenesis. Carcinogenesis. 1999; 20: 353–68.
26 Liu Y, Levy GN. Activation of heterocyclic amines by combinations of prostaglandin H synthase-1 and -2 with *N*-acetyltransferase 1 and 2. Cancer Lett. 1998; 133: 115–23.
27 Ames BN, Durston WE, Yamasaki E, Lee FD. Methods for detecting carcinogens with the *Salmonella*/mammalian-microsome mutagenicity test. Mutat Res. 1975; 31: 347–64.
28 Guengerich FP. Common and uncommon cytochrome P450 reactions related to metabolism and chemical toxicity. Chem Res Toxicol. 2001; 14: 611–50.
29 Paolini M, Cantelli-Forti G. On the metabolizing systems for short-term genotoxicity assays. Mutat Res. 1997; 387: 17–34.
30 Inami K, Ishikawa S, Mochizuki M. Mutagenicity of polyaromatic hydrocarbons by chemical models for cytochrome P450 in Ames assay. in press. Toxicol Environ Chem. 2009.
31 Inami K, Mochizuki M. Chemical models for cytochrome P450 as a biomimetic metabolic activation system in mutation assays. Mutat Res. 2002; 519: 133–40.
32 Inami K, Okazawa M, Mochizuki M. Mutagenicity of aromatic amines and amides with chemical models for cytochrome P450 in Ames assay. Toxicol in Vitro. 2009; 23: 986–91.
33 Haberle IB, Spasojevic I, Hambright P, Benov L, Crumbliss AL, Fridovich I. Relationship among redox potentials, proton dissociation constants of pyrrolic nitrogens, and *in vivo* and *in vitro* superoxide dismutating activities of manganese(III) and iron(III) water-soluble porphyrins. Inorg Chem. 1999; 38: 4011–22.
34 Maron DM, Ames BN. Revised methods for the *Salmonella* mutagenicity test. Mutat Res. 1983; 113: 173–215.
35 Inami K, Inokawa A, Sugita Y, Mochizuki M. Effect of substituted aryl group in water-soluble porphyrins on 2-aminofluorene activation in Ames assay. J Health Science. 2009; 55: 109–13.
36 Watanabe M, Ishidate Jr. M, Nohmi T. Sensitive method for the detection of mutagenic nitroarenes and aromatic amines: new derivatives of *Salmonella typhimurium* tester strains possessing elevated *O*-acetyltransferase levels. Mutat Res. 1990; 234: 337–48.
37 Shanabruch WG, Walker GC. Localization of the plasmid (pKM101) gene(s) involved in *recA*$^+$ *lexA*$^+$-dependent mutagenesis. Mol Gen Genet. 1980; 179: 289–97.
38 Wakabayashi K, Nagao M, Esumi H, Sugimura T. Food-derived mutagens and carcinogens. Cancer Res. 1992; 52: 2092s–8s.
39 Felton JS, Knize MG. Heterocyclic-amine mutagens/carcinogens in foods. In: Cooper CS, Grover PL, editors. Chemical Carcinogenesis and Mutagenesis I, Handbook of Experimental Pharmacology, Volume 94/I. Berlin: Springer-Verla; 1990. p. 471–502.
40 Salmeen IT, Foxall-VanAken S, Ball JC. A preliminary study of an iron porphyrin-iodosylbenzene system for activation of mutagens in Ames assay. Mutat Res. 1988; 207: 111–5.
41 Rueff J, Rodrigues A, Laires A, Gaspar J. Activation of promutagens by porphyrinic biomimetic systems. Mutat Res. 1992; 269: 243–50.
42 Inami K, Mochizuki M. Oxidative transformation of 2-acetylaminofluorene by a chemical model for cytochrome P450: a water-insoluble porphyrin and *tert*-butyl hydroperoxide. Bioorg Med Chem. 2008; 16: 7070–7.
43 Mansuy D, Bartoli J-F, Momenteau M. Alkane hydroxylation catalyzed by metalloporphyrins: evidence for different active oxygens species with alkylhydroperoxides and iodosobenzene as oxidants. Tetrahedron Lett. 1982; 23: 2781–4.

SAR and QSAR in Environmental Research
Vol. 21, Nos. 5–6, July–September 2010, 403–413

Taylor & Francis
Taylor & Francis Group

Development of an ecotoxicity QSAR model for the KAshinhou Tool for Ecotoxicity (KATE) system, March 2009 version

A. Furuhama[a]*, T. Toida[a], N. Nishikawa[a], Y. Aoki[a], Y. Yoshioka[b] and H. Shiraishi[a]

[a]*Research Center for Environmental Risk, National Institute for Environmental Studies (NIES), 16–2 Onogawa, Tsukuba 305–8506, Japan;* [b]*Faculty of Education and Welfare Science, Oita University, 700 Dannoharu, Oita 870–1192, Japan*

(*Received 18 February 2010; in final form 28 April 2010*)

The KAshinhou Tool for Ecotoxicity (KATE) system, including ecotoxicity quantitative structure–activity relationship (QSAR) models, was developed by the Japanese National Institute for Environmental Studies (NIES) using the database of aquatic toxicity results gathered by the Japanese Ministry of the Environment and the US EPA fathead minnow database. In this system chemicals can be entered according to their one-dimensional structures and classified by substructure. The QSAR equations for predicting the toxicity of a chemical compound assume a linear correlation between its log P value and its aquatic toxicity. KATE uses a structural domain called C-judgement, defined by the substructures of specified functional groups in the QSAR models. Internal validation by the leave-one-out method confirms that the QSAR equations, with $r^2 > 0.7$, RMSE ≤ 0.5, and $n > 5$, give acceptable q^2 values. Such external validation indicates that a group of chemicals with an in-domain of KATE C-judgements exhibits a lower root mean square error (RMSE). These findings demonstrate that the KATE system has the potential to enable chemicals to be categorised as potential hazards.

Keywords: QSAR; ecotoxicity prediction; classification; chemical substances; domain; KATE

1. Introduction

Quantitative structure–activity relationships (QSARs) are potential tools for predicting the activity and properties of chemicals, including their physicochemical attributes, health effects, ecotoxicity and biological activity. QSAR models can estimate and predict such activity and can thus be used to categorise chemicals in terms of their potentially hazardous nature. A recent review has demonstrated that acute aquatic toxicity [1] can be predicted using QSAR and describes the available databases of ecotoxicity data.

Prediction of toxicity by QSAR does not require lengthy experiments, nor the use of animals, plants or cells. QSAR models have therefore been utilised for the assessment of new and existing chemicals for conformity with regulatory requirements in countries within the Organisation for Economic Co-operation and Development (OECD) [2]. In Japan, under the Chemical Substances Control Law (CSCL), the Ministry of the Environment (MoE) is responsible for evaluating the adverse effects of chemicals on

*Corresponding author. Email: ayako.furuhama@nies.go.jp

ISSN 1062–936X print/ISSN 1029–046X online

DOI: 10.1080/1062936X.2010.501815
http://www.informaworld.com

ecosystems, and uses tests involving aquatic organisms such as *Oryzias latipes* (fishes) or *Daphnia magna* (daphnia), in addition to algae data available from the MoE website [3]. The Japanese National Institute for Environmental Studies (NIES) was established to apply QSAR models to acute ecotoxicity, and has developed a QSAR prediction system using the MoE ecotoxicity database. This system, published in March 2009, is known as the *KAshinhou Tool for Ecotoxicity* (KATE) [4].

The present paper focuses on the theoretical and methodological aspects of the KATE system, and QSAR equations classified by chemical substructure are introduced. We shall then present the cross-validation ('leave-one-out') results, and the toxicities calculated by KATE, and by alternative systems such as TIssue MEtabolism Simulator (TIMES) [5,6] (developed by Zlatarov at the Laboratory of Mathematical Chemistry, Bourgas University, Bulgaria), and by ECOSAR™ [7] (developed by the US Environmental Protection Agency (EPA)) using the same end-point data set as that in KATE. The validity of KATE will be discussed using the applicability domain, log P, and C-judgements.

2. Overview of KATE

2.1 *End-point*

KATE uses experimental data on chemical substances to predict aquatic toxicity. The end-points of interest are the 96-hour median lethal concentration (LC_{50}) in fish after acute toxicity tests, and the 48-hour median effective concentration (EC_{50}) in daphnia obtained after acute immobilisation tests. Training sets for QSAR development were derived from the results of ecotoxicity tests (*Oryzias latipes* LC_{50} and *Daphnia magna* EC_{50}) obtained by the MoE [3], as well as the results of acute toxicity tests from the US EPA fathead minnow (*Pimephales promelas*) database [8,9]. In the KATE system, the 96-hour LC_{50} data for *Oryzias latipes* and fathead minnow were combined to reinforce the number of reference datasets. The QSAR equations in KATE for the fish and daphnia end-points were designed using 535 and 258 chemicals, respectively.

2.2 *Classification of chemicals*

Chemical substances can be classified according to the substructures that give rise to specific chemical properties (Appendix 1 of the supplementary material which is available on the Supplementary Content tab of the article's online page at http://dx.doi.org/10.1080/1062936X.2010.501815). The rules for daphnia and fish end-points are identical, except for the following five classes: *amines aromatic or phenols1*, *amines aromatic or phenols3*, *amines aromatic or phenols4*, *amines aromatic or phenols5*, and *primary amines*. According to KATE, the toxicity of a chemical containing amino functional groups might be different in daphnia from its toxic behaviour in fish.

Forty-four classes are proposed for each end-point of KATE QSAR models. Table 1 shows the QSAR class name, and the detailed class features are listed in Appendix 2 of the supplementary material (available online). The chemicals in the KATE *unclassified* class were not categorised within any of the rules in Appendix 2. Additional classification rules or fragment definitions are required in further studies to reduce the number of chemicals described as *unclassified*. It should be noted that the concept of *unclassified* within KATE does not always include reactive chemicals, and thus differs from the *reactive unspecified* category in the TIMES software.

Table 1. QSARs for fish acute toxicity estimated by the equation: $\log(1/LC_{50}[\mathrm{mM}]) = a * \log \mathrm{P} + b$.

Class name	*a, b*	*n*	*RMSE*	r^2, q^2	*log P range*	*1
Hydrocarbons aromatic	0.630, −0.883	43	0.368	0.826, 0.803	[0.60, 5.17]	
Dinitrobenzenes	0.568, 0.551	12	0.669	0.331, 0.170	[0.56, 3.60]	
Nitrobenzenes	0.678, −0.693	9	0.300	0.875, 0.760	[0.82, 5.10]	
Amines aromatic or phenols1	−0.005, 2.671	7	0.354	0.001, 0.887	[−0.30, 4.47]	
Amines aromatic or phenols2	0.012, 1.863	7	0.307	0.003, 0.737	[3.67, 8.47]	C
Amines aromatic or phenols3	0.214, 0.945	16	0.305	0.272, 0.106	[0.15, 3.68]	
Amines aromatic or phenols4	0.725, −0.779	56	0.321	0.900, 0.890	[0.51, 7.54]	
Amines aromatic or phenols5	0.544, −0.612	22	0.324	0.661, 0.600	[0.35, 3.50]	
Primary amines	0.529, −0.622	23	0.406	0.803, 0.741	[−2.04, 3.60]	
Secondary and tertiary amines	0.592, −0.595	10	0.512	0.731, 0.605	[−1.43, 2.79]	C
Hydrazines	0.417, 1.832	4	0.413	0.884, 0.639	[−1.68, 4.70]	
Amides and imides	0.746, −1.026	17	0.601	0.696, 0.607	[−0.48, 3.80]	
Esters aliphatic	0.638, −0.600	13	0.393	0.722, 0.651	[0.18, 3.65]	
Esters aromatic	0.513, −0.157	9	0.253	0.856, 0.790	[1.94, 5.53]	
Aldehydes	0.484, 0.279	15	0.557	0.272, 0.111	[−0.34, 2.47]	
Acids	0.728, −1.652	9	0.355	0.816, 0.667	[0.33, 4.20]	
Acids acrylic	0.122, 0.045	3	0.039	0.607, 0.271	[0.35, 1.33]	
Conjugated systems1	0.753, 2.084	4	1.012	0.463, 0.111	[−1.11, 2.20]	
Conjugated systems2	0.436, 0.901	17	1.007	0.264, 0.066	[−0.38, 4.10]	
Thiols aromatic	NO-QSAR					
Thiols aliphatic	0.371, 0.732	4	0.291	0.910, 0.633	[−0.17, 6.12]	C
Sulfides	0.753, −1.336	8	0.259	0.699, 0.573	[2.46, 4.16]	C
Disulfides	0.386, 0.845	6	0.666	0.210, 0.012	[1.74, 4.44]	C
Carbamates	0.004, 1.894	11	0.519	0.000, 0.645	[−0.47, 4.60]	
Pyrethroids	NO-QSAR					
Acrylates	0.158, 1.498	6	0.155	0.474, 0.022	[−0.21, 2.36]	
Methacrylates	0.465, −0.031	6	0.417	0.657, 0.293	[0.47, 4.54]	
Epoxides	0.323, 1.055	4	0.272	0.755, 0.283	[0.08, 3.98]	C
Barbitals or thiols other	1.583, −2.560	4	0.291	0.657, 0.927	[1.47, 2.10]	
Esters phosphate	0.691, −0.111	11	0.856	0.389, 0.175	[2.23, 5.33]	
N or P cations	0.274, 0.956	9	0.579	0.791, 0.628	[−8.36, 6.69]	C
Halides1	0.254, 1.325	6	0.971	0.112, 0.078	[0.45, 4.50]	
Halides2	0.824, −0.318	8	0.560	0.879, 0.810	[−0.06, 5.04]	
Halides3	0.783, −1.291	42	0.263	0.879, 0.868	[1.25, 4.89]	
Metals	NO-QSAR					
Nitriles aliphatic	0.839, −1.154	6	0.254	0.938, 0.901	[−0.34, 3.12]	N
Ketones	0.864, −1.602	21	0.345	0.891, 0.867	[−0.24, 4.09]	N
Alcohols or ethers aliphatic	0.853, −1.958	23	0.321	0.950, 0.924	[−0.77, 5.82]	N
Phosphates	0.891, −1.926	3	0.257	0.865, 0.485	[2.83, 4.59]	N
Hydrocarbons aliphatic	0.753, −1.286	15	0.289	0.824, 0.785	[2.42, 5.56]	N
Ethers aliphatic	0.749, −1.806	11	0.190	0.972, 0.962	[−0.54, 4.25]	N
Ethers aromatic	0.870, −1.466	10	0.233	0.922, 0.892	[1.16, 4.21]	N
Neutral organics	0.842, −1.674	88	0.384	0.924, 0.919	[−0.77, 5.82]	
Unclassified	0.744, −0.898	25	0.714	0.712, 0.660	[−1.35, 5.50]	

*1 C: an equation is generated by calculated Clog *P*. N: a member of the *Neutral organics* class.
Note: *n*, RMSE, r^2 and q^2 denote the number of chemicals in a class, the root mean square error, the squared correlation coefficient, and the leave-one-out version of the squared correlation coefficient, respectively. The log *P* range shows minimum and maximum log *P* values.

2.3 *Neutral organics*

Neutral organics is an aggregate of the chemicals in defined classes in the KATE system. It comprises the classes: *nitriles aliphatic*, *ketones*, *alcohols or ethers aliphatic*, *phosphates*, *hydrocarbons aliphatic*, *ethers aliphatic* and *ethers aromatic*. In the OECD Environment Monograph [10], *neutral organic* compounds of minimal toxicity were divided into the groups: *aliphatic alcohols*, *aliphatic ketones*, *aliphatic ethers* and *alkoxyethers*, *aliphatic halogenated hydrocarbons*, *saturated alkanes* and *halogenated benzenes*. Some of the *neutral organics* compounds defined in the OECD monograph were categorised differently from those in KATE.

2.4 *QSAR equations*

The QSAR equations in the KATE model express the correlation between the octanol/water partition coefficient (log P) of a compound and its aquatic toxicity, using simple linear regression analysis. Measured log P values were used to derive the QSAR equations, except for the equations labelled C in Tables 1 and 2. In cases where experimental log P values were not available, an equation was constructed from the calculated Clog P value obtained by the Daylight toolkit [11]. The LC_{50} and EC_{50} values in the equation were expressed in terms of the common logarithm of the inverse of millimoles per litre (mmol L^{-1}, or mM). The equations and the statistical information obtained are shown in Tables 1 and 2. Where there were fewer than three sets of reference data within one class, QSAR prediction could not be performed. In such cases the class name was the only information obtained from KATE, and the label NO-QSAR is indicated in Tables 1 and 2. The equation for a class named *pyrethroids* was not constructed, since the log P values in the reference data were gathered in higher ranges [6.1, 6.5].

2.5 *Domains in KATE*

KATE offers two 'judgements' to verify whether or not a predicted chemical substance falls within the applicability domain of a QSAR class. The first is the log P judgement, based on the log P range defined by the reference chemical data of the class concerned. This has been categorised as a descriptor domain [12,13]. The interpolated log P range for each class is listed in Tables 1 and 2.

The second is the C-judgement, which is categorised as a structural domain and is defined by the substructures shown in Appendix 3 of the supplementary material (available online). The substructures are based on functional groups having similar concepts to those used by Schultz et al. [13], rather than on atom-centred fragments [12,14]. Schultz et al. applied the structural domain to one QSAR equation for aromatic compounds, and the out-of-domain revealed well-known electrophoric mechanisms in the structural space(s) [13]. In the KATE system the classification rules (described in Section 2.2) play a role in constructing such structural space(s). The definition of the applicability domain of C-judgement depends on whether all the substructures of the chemical under test are found in reference chemicals in the class, or secondly, whether all substructures in the test chemical are present in reference chemicals in either *neutral organics* or the class concerned. The first of these definitions is stricter than the second. The reliability of the log P and C-judgements is assessed later in Section 4 (Results and discussion).

Table 2. QSARs for the daphnia acute toxicity estimated by the equation: $\log(1/EC_{50}[\mathrm{mM}]) = a * \log P + b$.

Class name	*a, b*	*n*	*RMSE*	r^2, q^2	*log P range*	*1
Hydrocarbons aromatic	0.607, −0.414	26	0.351	0.808, 0.762	[0.65, 5.17]	
Dinitrobenzenes	0.408, 0.632	5	0.561	0.343, 0.090	[0.56, 3.60]	
Nitrobenzenes	0.547, −0.164	4	0.238	0.915, 0.675	[1.17, 5.10]	
Amines aromatic or phenols1	0.085, 2.441	7	0.443	0.057, 0.375	[−0.33, 3.41]	
Amines aromatic or phenols2	0.097, 1.152	6	0.277	0.239, 0.031	[3.67, 8.47]	C
Amines aromatic or phenols3	0.132, 1.748	16	0.406	0.119, 0.018	[0.04, 3.91]	
Amines aromatic or phenols4	0.576, −0.042	28	0.297	0.838, 0.814	[1.32, 6.06]	
Amines aromatic or phenols5	0.552, 0.114	12	0.260	0.802, 0.728	[1.18, 3.91]	
Primary amines	0.189, −0.059	4	0.248	0.390, 0.095	[−1.31, 1.49]	
Secondary and tertiary amines	0.133, 0.200	4	0.150	0.517, 0.040	[−1.50, 1.45]	
Hydrazines	0.190, 1.987	5	0.289	0.766, 0.360	[−2.46, 4.70]	C
Amides and imides	0.212, 0.585	8	0.593	0.151, 0.135	[0.23, 3.80]	
Esters aliphatic	0.666, −0.819	6	0.324	0.927, 0.762	[0.25, 5.41]	
Esters aromatic	0.459, −0.417	3	0.010	1.000, 0.998	[1.60, 4.72]	
Aldehydes	0.521, 0.295	5	0.555	0.616, 0.084	[0.42, 4.47]	C
Acids	0.222, −0.113	7	0.644	0.133, 0.298	[0.08, 4.20]	
Acids acrylic	0.057, 0.248	3	0.143	0.025, 0.947	[0.35, 1.33]	
Conjugated systems1	0.630, 1.393	5	0.321	0.957, 0.916	[−1.76, 4.65]	C
Conjugated systems2	0.213, 0.906	11	0.775	0.097, 0.047	[0.17, 3.70]	
Thiols aromatic	NO–QSAR					
Thiols aliphatic	0.427, 1.410	4	0.786	0.647, 0.049	[−0.17, 6.12]	C
Sulfides	NO–QSAR					
Disulfides	1.041, −0.724	3	0.480	0.865, 0.635	[1.74, 4.44]	C
Carbamates	0.046, 2.991	4	0.688	0.008, 0.523	[0.94, 4.60]	
Pyrethroids	NO–QSAR					
Acrylates	0.003, 1.401	4	0.069	0.002, 0.646	[−0.21, 2.36]	
Methacrylates	0.461, −0.422	5	0.301	0.824, 0.653	[0.47, 4.54]	
Epoxides	0.486, 0.589	4	0.341	0.817, 0.598	[0.08, 3.98]	C
Barbitals or thiols other	NO–QSAR					
Esters phosphate	2.133, −2.376	3	1.477	0.204, 0.526	[3.08, 3.88]	
N or P cations	NO–QSAR					
Halides1	−0.665, 4.825	3	0.350	0.800, 0.998	[2.09, 4.50]	
Halides2	0.880, −0.317	4	0.552	0.860, 0.494	[1.10, 5.04]	
Halides3	0.826, −1.008	24	0.237	0.901, 0.883	[1.47, 4.73]	
Metals	NO–QSAR					
Nitriles aliphatic	NO–QSAR					N
Ketones	NO–QSAR					N
Alcohols or ethers aliphatic	0.641, −1.053	6	0.214	0.958, 0.923	[1.10, 5.82]	N
Phosphates	0.579, −0.634	3	0.103	0.983, 0.922	[1.44, 4.59]	N
Hydrocarbons aliphatic	0.660, −0.555	10	0.268	0.891, 0.797	[2.42, 6.54]	N
Ethers aliphatic	NO–QSAR					N
Ethers aromatic	0.492, 0.285	4	0.437	0.406, 0.088	[2.16, 4.21]	N
Neutral organics	0.696, −0.870	26	0.418	0.857, 0.835	[0.68, 6.54]	
Unclassified	0.537, 0.078	12	1.097	0.475, 0.287	[−1.02, 5.50]	

*1 *C*: an equation is generated by the calculated Clog *P*. N: a member of the *Neutral organics* class. Note: *n*, RMSE, r^2, and q^2 denote the number of chemicals in a class, the root mean square error, the squared correlation coefficient, and the leave-one-out version of the squared correlation coefficient, respectively. The log *P* range shows minimum and maximum log *P* values.

2.6 *KATE system software*

The KATE software was first made available to the public in January 2008. An updated version of KATE, including standalone personal computer and internet versions, was released in March 2009. The standalone version, called 'KATE on PAS', and the internet version, called 'KATE on NET', adopted the KOWWIN^{TM} [15] of the US EPA, and Clog P [11] estimated by the Daylight system, respectively, to estimate the calculated log P. Except for the treatment of calculated log P values, KATE on PAS and KATE on NET use the same classification algorithm, *fragment identification by tree structure* (FITS), developed by Yoshioka.

In the KATE system, the input is *simplified molecular input line entry specification* (SMILES) and log P (if available) for toxicity prediction, and the output is the calculated toxicity concentration (LC_{50} or EC_{50}), the QSAR class found for the predicted chemical, and the domain judgements. If the measured log P of a chemical is not available, the calculated log P according to the SMILES information (KOWWIN or C log P) is adopted.

3. Methods of QSAR validation

First, leave-one-out cross validations were examined for training sets used in the QSAR equations of KATE. Secondly, external validations were performed using test set compounds not included in the KATE training sets due to lack of measured log P values. The 287 fish 96-hour LC_{50} and 98 daphnia 48-hour EC_{50} from the Japan MoE, along with the US EPA fathead minnow database, were used for comparison of the calculated toxicity by the KATE software version published in March 2009, TIMES v. 2.25, and ECOSAR v. 0.99 h (1999).

It is worth mentioning that the end-points of the data calculated by KATE were not identical to those calculated by TIMES and ECOSAR. Fish (mixed with *Oryzias latipes* and fathead minnow acute toxicity tests) 96-hour LC_{50} and daphnia 48-hour EC_{50} (KATE), *Pimephales promelas* 96-hour LC_{50} and daphnia 48-hour EC_{50} (TIMES), and fish 96-hour LC_{50} and daphnia 48-hour LC_{50} (ECOSAR) were therefore adopted. The input of KATE and ECOSAR were SMILES strings, and calculated log P by KOWWIN. In TIMES, only the lists of SMILES strings were used as input values, and quantum chemical calculations were performed using MOPAC AM1 Hamiltonian, using the 'precise' option, without taking other conformers into account.

4. Results and discussion

4.1 *Cross validation*

The QSAR equations were validated by the leave-one-out method obtained from the KATE system. The complete list of results is given in Appendix 4 of the supplementary material (available online). The statistical data are displayed in Tables 1 and 2. The criterion proposed by Hulzebos and Posthumus [16] was evaluated, in which the estimations from models should not deviate from the experimental value by a factor of 10 or above. For fish, 575 of the 628 chemicals met the acceptable criteria, and for daphnia 241 of 290 did so. (In this instance the 628 and 290 chemicals involved some degree of duplication.) Using the QSAR equations in the KATE system, more than 80% of chemicals were predicted within a factor of 10. The classes with less than a 0.7 squared correlation coefficient ($r^2 < 0.7$), and/or more than 0.5 RMSE, tended to increase the